

# Site Classification using Feed Forward Backpropagation Artificial Neural Networks.

Ebru Efeoğlu<sup>1\*</sup>

<sup>1\*</sup>Software Engineering/ Engineering Faculty, Kütahya Dumlupınar University, Kütahya, Turkey ([ebru.efeoglu@dpu.edu.tr](mailto:ebru.efeoglu@dpu.edu.tr)) (ORCID: 0000-0001-5444-6647)

**Abstract** – Strong rock is less affected by the waves propagating during an earthquake. For this reason, structures on strong rocks are less affected by earthquakes. Identifying strong rocks is important for a safe residential area. There are different earthquake codes declaring the characteristics of strong rocks. In this study, site classification was made according to four different earthquake Provisions Nehr, TBDY, Rm, E code. Feed Forward Backpropagation Artificial Neural Networks was used for site classification. Shear wave velocity (V<sub>30</sub>), Ground dominant period (T<sub>0</sub>) and H/V ratio were selected as input parameters to this network. Performance analysis was performed to determine which regulation of the Feed Forward Backpropagation Artificial Neural Networks algorithm made the classification more successful. The cross-validation method was used for the analysis. Accuracy, Precision Recall, Kappa, Area under the ROC Curve (AUC) and Root Mean Squared Error (RMS) error values were calculated. As a result, 98% accuracy value was obtained after cross validation in strong rock detection according to E-Code-8 regulation. According to this regulation, all metric values calculated in strong rock detection are higher than other regulations. In addition, hard rock was detected with the least error rate according to this regulation.

**Keywords** – Strong Rock, Nehr, TBDY, Rm, E-code, Feed Forward Backpropagation Artificial Neural Networks.

**Citation:** Efeoğlu, E., (2023). Site Classification using Feed Forward Backpropagation Artificial Neural Networks. International Journal of Multidisciplinary Studies and Innovative Technologies, 7(2): 41-46.

## I. INTRODUCTION

Earthquakes are natural disasters that cause the death of many people and the destruction of buildings. During an earthquake, seismic waves are propagated. Soil characterization is essential in defining the seismic effect. It is necessary to minimize the damage caused by earthquakes. Adequate knowledge of the physical and mechanical properties of the soil is required in order to design buildings both reliably and economically. At the same time, it is necessary to know the structure of the ground well in order to take precautions for problems such as liquefaction, swelling, landslide. Data obtained by using geophysical test methods should be evaluated while making soil classifications. Türkiye is in an earthquake zone. For example, although it was a medium-sized earthquake, many people died in the Dinar earthquake. Many studies were carried out in the earthquake zone. It was concluded that the main causes of damage were poor ground conditions.

The shear wave velocity is used to evaluate the dynamic behavior of shallow underground soil. In soil characterization, near-surface shear wave velocity values are generally used. The average shear wave velocity for the top 30 m of soil is called VS<sub>30</sub>. VS<sub>30</sub> values were calculated using multi-channel surface waves analysis (MASW) in Dinar and a soil classification map was created (1).

Some additional information regarding the properties of passive surface wave data and their use in the H/V spectral ratio technique was discussed (2) Site characterization with

seismic noise in Istanbul, Turkey (3) A preliminary microzonation based on liquefaction potential was performed for Ceyhan District of Adana (4). A local field impact assessment (6) was performed for the Bornova Plain (İzmir, Turkey) and its surroundings (5) using the HVSr (Nakamura technique) and MASW methods for Aliğa/İzmir. The importance of Soil and Geological Features in City Planning was emphasized (7). Turkey's strong movement site conditions (8), geophysical and geotechnical studies were used to determine site classification. (9). Shear wave velocity profiles of the Hatay were determined by MASW and ReMi techniques. Transfer functions (maximum H/V amplitude ratios) and dominant periods were obtained by applying microtremor studies at the same locations (10). After applying the SMOTE (Synthetic Minority Over-Sampling Technique) process to these data, it was used as an input to the neural networks.

Soil classification criteria and local soil classes are defined in various regulations. In this study, NEHRP Provisions (11), Eurocode-8 (12), Turkey Building Earthquake Code (TBDY-2018) (13) and Rodriguez-Marek et al. Soils were classified according to (14). Geophysical Problems and Possible Solutions in Soil Classification Based on Eurocode 8 were discussed (15). Artificial neural networks have previously been used to predict the stability of soil and rock slope (16), to estimate the consolidation coefficient (17), to predict the swelling strength of large soils (18) and to estimate rock tension using deep neural networks (19).

**II. MATERIALS AND METHOD**

Multilayer perceptron( MLP) networks work according to the learning strategy. In other words, these networks are given both inputs and (expected) outputs that must be produced in response to the inputs during training. The task of the network is to generate the output corresponding to that input for each input. The learning rule of the MLP network is the Delta learning rule based on the least squares method. A set of examples is needed in education. For each sample in this set, both the inputs and the outputs that the network should produce for the inputs must be determined.

The delta rule consists of two phases. These are the forward calculation phase and the backward calculation phase.

In the forward computation phase, a sample in the training set comes to the input layer. There is no information processing in this layer. Inputs are processed in the middleware. The Sigmoid function is generally used as the activation function. The values that come out of the output layer are the outputs of the network. When these outputs are obtained, the advanced calculation is completed. In backward computation, the output produced by the network for the input presented to the network is compared with the expected outputs of the network. The difference between them is considered an error. By distributing this error to the weight values, the error is reduced in the next iteration. The purpose of training the MLP network is to minimize this error. The weights of the process elements are changed to minimize the total error.

In the study, the Sigmoid function was used on the nodes in all networks.

The formulas of the performance metrics used in the study are given in Equation (1,2,3,4,5,6,7), respectively.

$$\text{Accuracy} = \frac{CTP+CTN}{TP+TN+FP+FN} \tag{1}$$

$$\text{Precision} = \frac{CTP}{CTP+CFP} \tag{2}$$

$$\text{Recall} = \frac{CTP}{CTP+CFN} \tag{3}$$

$$F - \text{Measure} = 2 \times \frac{(\text{Precision} \times \text{Recall})}{(\text{Precision} + \text{Recall})} \tag{4}$$

$$TPR = \frac{CTP}{CFP+CTN} \tag{5}$$

$$TNR = \frac{CTN}{CTP+CFN} \tag{6}$$

$$\text{Kappa} = \frac{P(i)-P(j)}{1-P(j)} \tag{7}$$

Where, P(i) refers to the accuracy of the algorithm, P(j) refers to the weighted average of the expected accuracy of the algorithm that makes random predictions on the same dataset. The number of samples that Artificial Neural Networks (ANN) predicted correctly in the equations is represented by Classification true positive (CTP) and Classification true negative (CTN), and the number of misclassified samples is represented by Classification false positive (CFP) and Classification false negative (CFN).

TPR and FPR values were used in the drawing of the Roc curve and the area under the ROC curve AUC) value was calculated.

The success of the classification depends on these metrics being close to 1. Because metrics take a maximum value of 1, which means perfect classification.

In the classification, Shear wave velocity (V30), Ground dominant period (To) and H/V ratio were given as input parameters to the network. Then, classes were determined separately according to each regulation.

**III. RESULTS**

First, three area classes (B, C, D) were determined for site classification according to the NEHRP provisions. The network is then trained. The cross validation method was used to test the algorithm. The generated network model is given in Fig. 1, and the confusion matrices obtained after training and cross-validation are given in Fig. 5.

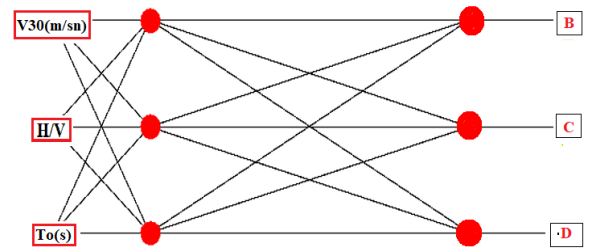


Fig. 1. Network created according to Nehrp

According to TBDY provisions, 3 classes (ZB, ZC, ZD) were determined for site classification. The model of the network is given in Fig.2 and the confusion matrix after training and cross-validation is given in Fig.6.

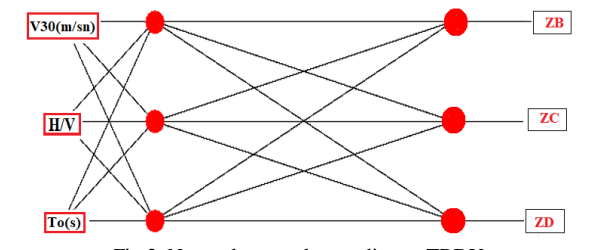


Fig 2. Network created according to TBDY

According to Ecode provisions, 3 classes (A, B,C) were determined for site classification. The model of the network is given in Fig.3 and the confusion matrix after training and cross-validation is given in Fig.7.

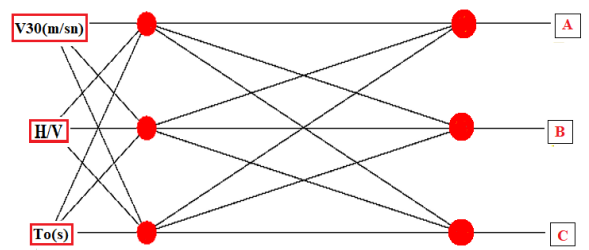


Fig 3. Network created according to Ecode

According to Rm provisions, 6 classes (C-1, C-2, D-1, D-2, D-3) were determined for site classification. The model of the network is given in Fig.4 and the confusion matrix after training and cross-validation is given in Fig.8.

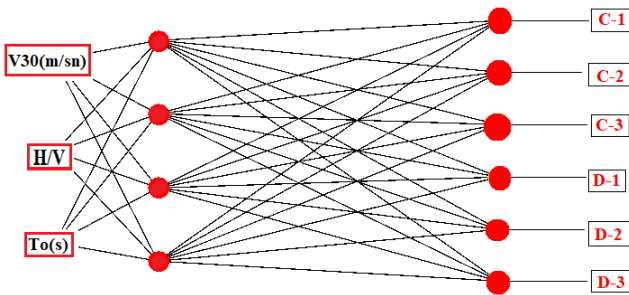


Fig 4. Network created according to Rm

In all earthquake Regulation, the strong site is represented by the first letters of the alphabet. Towards the end of the alphabet, the site is more loose and earthquake-resistant. For example, the strong site is represented by A according to Ecode, ZB according to TBDY, B according to Nehrp, C-1 according to Rm.

|              |   | Predicted class |    |    |                  |    |    |
|--------------|---|-----------------|----|----|------------------|----|----|
|              |   | Training        |    |    | Cross validation |    |    |
| Actual class |   | B               | C  | D  | B                | C  | D  |
|              | B | 16              | 0  | 0  | 16               | 0  | 0  |
|              | C | 0               | 16 | 0  | 0                | 15 | 1  |
|              | D | 0               | 0  | 16 | 0                | 1  | 15 |

Fig 5. The confusion matrix of the network created according to Nehrp

According to Fig 5, all the instances were correctly classified in the training according to the Nehrp provisions. In cross validation, one class C instance and one class D instance were incorrectly classified.

|              |    | Predicted class |    |    |                  |    |    |
|--------------|----|-----------------|----|----|------------------|----|----|
|              |    | Training        |    |    | Cross validation |    |    |
| Actual class |    | ZB              | ZC | ZD | ZB               | ZC | ZD |
|              | ZB | 16              | 0  | 0  | 16               | 0  | 0  |
|              | ZC | 0               | 16 | 0  | 0                | 13 | 3  |
|              | ZD | 0               | 0  | 16 | 0                | 1  | 15 |

Fig 6. The confusion matrix of the network created according to TBDY

According to Fig 6., all the instances were correctly classified in the training according to the TBDY provisions. In cross validation, one class ZD instance and three class ZC instance were incorrectly classified.

|              |   | Predicted class |    |    |                  |    |    |
|--------------|---|-----------------|----|----|------------------|----|----|
|              |   | Training        |    |    | Cross validation |    |    |
| Actual class |   | A               | B  | C  | A                | B  | C  |
|              | A | 17              | 0  | 0  | 17               | 0  | 0  |
|              | B | 0               | 17 | 0  | 0                | 16 | 1  |
|              | C | 0               | 0  | 17 | 0                | 0  | 17 |

Fig 7. The confusion matrix of the network created according to E-Code

According to Fig 7, all the instances were correctly classified in the training according to the E-Code provisions. In cross validation, only one instance were incorrectly classified.

|              |     | Predicted class |     |     |     |     |     |
|--------------|-----|-----------------|-----|-----|-----|-----|-----|
|              |     | Training        |     |     |     |     |     |
| Actual class |     | C-1             | C-2 | C-3 | D-1 | D-2 | D-3 |
|              | C-1 | 11              | 0   | 0   | 0   | 0   | 0   |
|              | C-2 | 0               | 11  | 0   | 0   | 0   | 0   |
|              | C-3 | 0               | 0   | 11  | 0   | 0   | 0   |
|              | D-1 | 1               | 0   | 0   | 8   | 2   | 0   |
|              | D-2 | 0               | 0   | 0   | 0   | 11  | 0   |
|              | D-3 | 0               | 0   | 0   | 0   | 0   | 11  |

|              |     | Cross validation |     |     |     |     |     |
|--------------|-----|------------------|-----|-----|-----|-----|-----|
| Actual class |     | C-1              | C-2 | C-3 | D-1 | D-2 | D-3 |
|              | C-1 | 11               | 0   | 0   | 0   | 0   | 0   |
|              | C-2 | 0                | 11  | 0   | 0   | 0   | 0   |
|              | C-3 | 0                | 0   | 11  | 0   | 0   | 0   |
|              | D-1 | 0                | 0   | 1   | 4   | 3   | 2   |
|              | D-2 | 0                | 0   | 1   | 1   | 8   | 1   |
|              | D-3 | 0                | 0   | 0   | 0   | 0   | 11  |

Fig 8. The confusion matrix of the network created according to Rm

According to Fig 8, In training, two class instances were incorrectly classified. In cross validation, nine instances were incorrectly classified.

Performance evaluation of different classifications in both training and cross validation, Precision, Recall, F-measure, AUC, Kappa and Rms values were calculated. The graphs of these values are given in Fig.9, 10, 11, 12, 13, 14, 15.

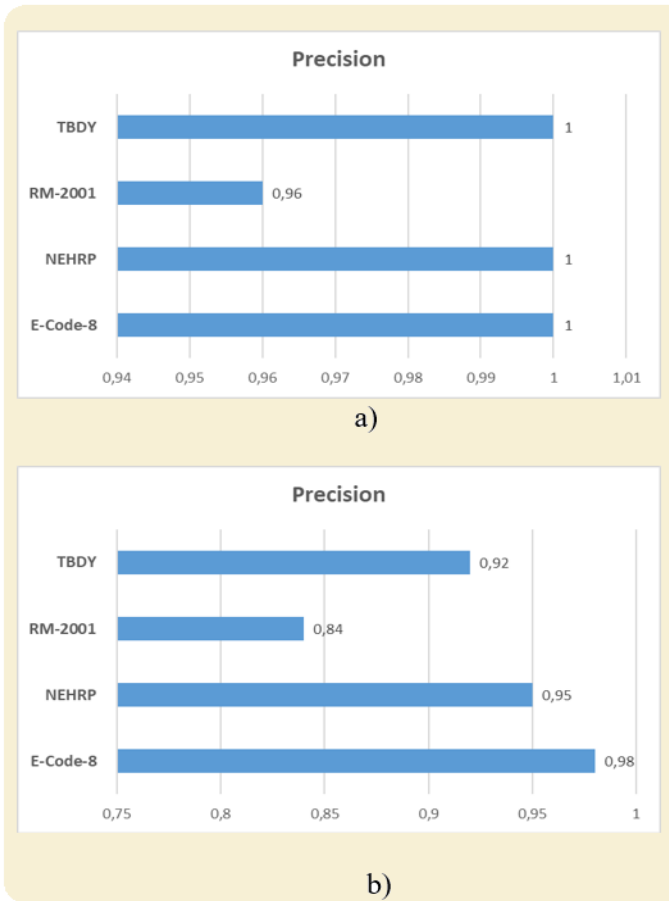


Fig 9. Precision values a)Training b)Cross validation

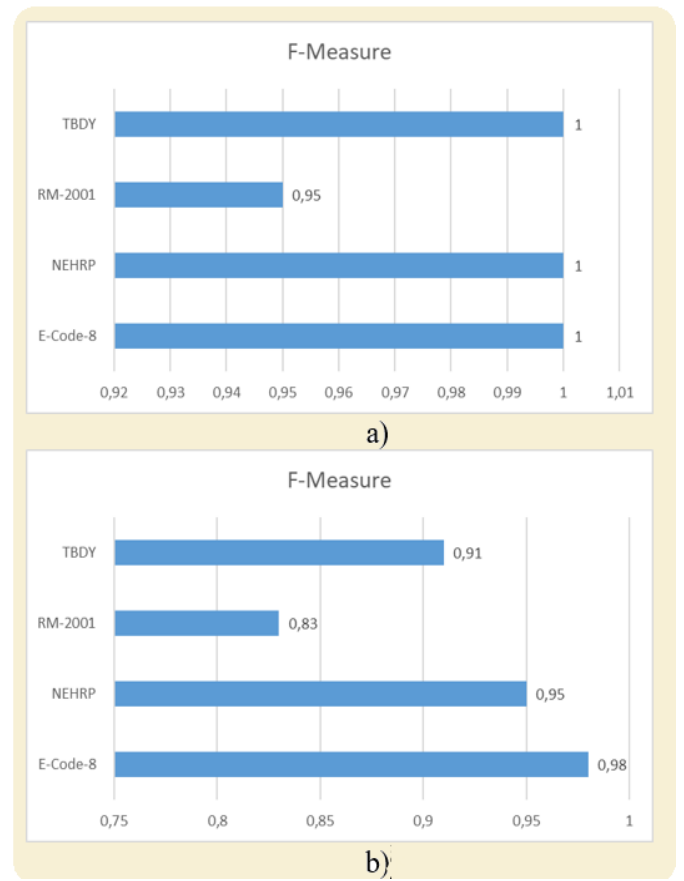


Fig 11. F-Measure values a)Training b)Cross validation

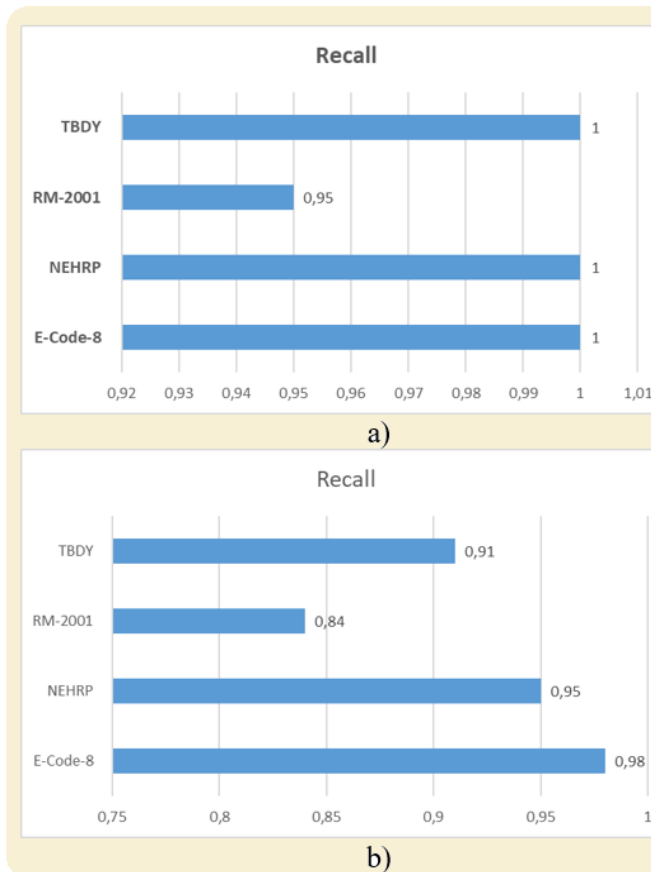


Fig 10. Recall values a)Training b)Cross validation

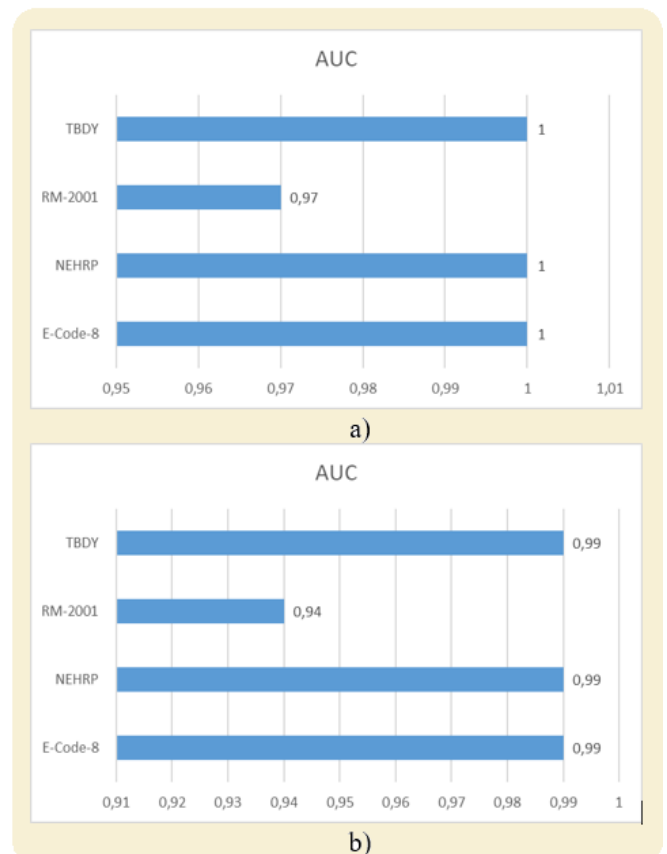


Fig 12. AUC values a)Training b)Cross validation

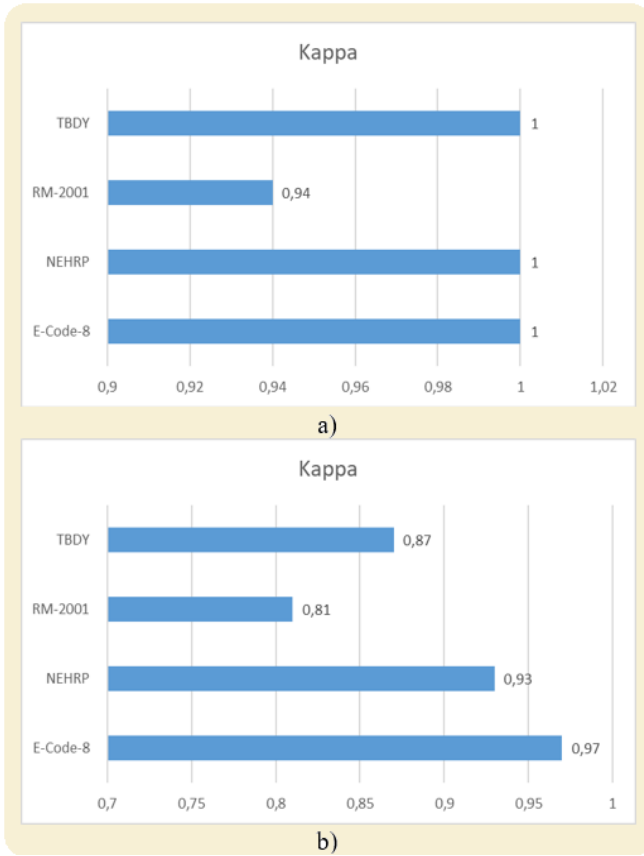


Fig 13. Kappa values a)Training b)Cross validation

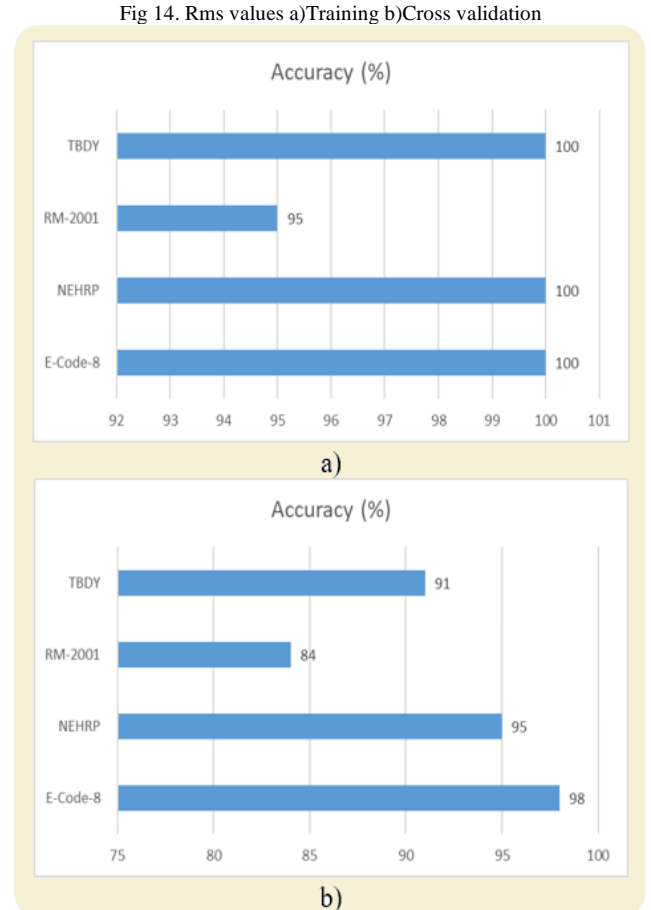
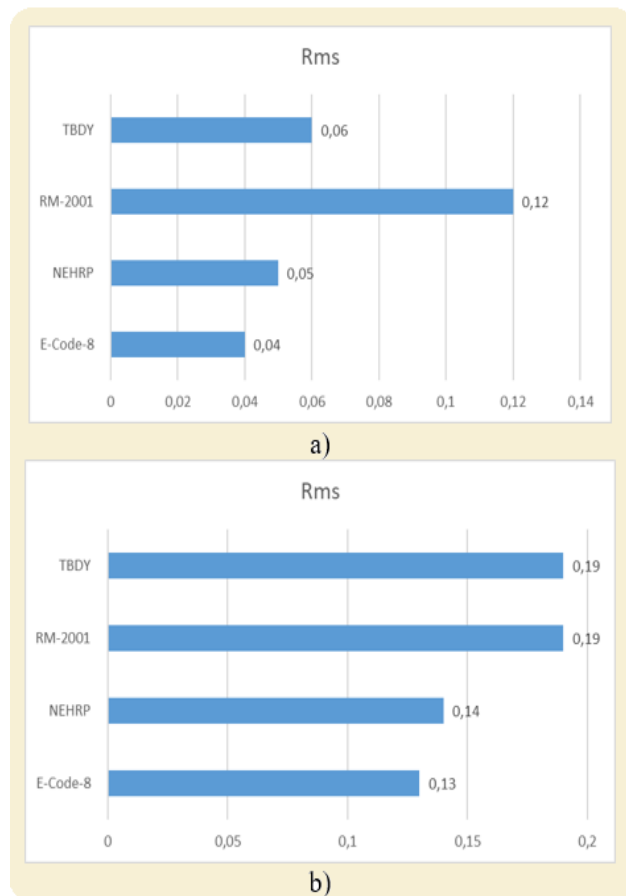


Fig 14. Rms values a)Training b)Cross validation



In successful classification, all other metrics except the Rms value are required to be 1 or close to 1. When the data set was classified according to Rm, the lowest performance metrics were obtained. Higher metric values were calculated when classified according to other regulations. When the Rms values were compared, the highest Rms value was calculated when the data set was classified according to Rm.

#### IV. DISCUSSION CONCLUSION

Especially in countries located in the earthquake zone, deaths and damages should be prevented. It is possible to prevent these damages by building a structure suitable for the ground. For example, there is a danger of liquefaction during an earthquake in very loose and sandy soils. For this reason, effects such as collapse, sliding and overturning are frequently seen in the structures. Suitable for hard site construction whenever possible.

This study is important for reducing earthquake damage and for a reliable construction. The sites were classified using data obtained by geophysical methods. These classifications were made according to different regulations. Limited data were used. It is planned to carry out a more detailed study by increasing the number of data in future studies. In the study, the site classification of Hatay province was made according to different regulations. Feed Forward Backpropagation Artificial Neural Networks was used. As a result, the highest metric values were calculated in the classifications according to the E-code regulation. Therefore, the most successful classification is configured according to the E-code regulation.

The accuracy of this classification is 100% in training, 98% in cross validation. It was also classified with the lowest error. The Rms error rate is 0.04 in training and 0.13 in cross validation.

### Statement of Conflicts of Interest

There is no conflict of interest between the authors.

### Statement of Research and Publication Ethics

The authors declare that this study complies with Research and Publication Ethics

### REFERENCES

- [1] Kanlı, A. I., Tildy, P., Prónay, Z., Pınar, A., & Hermann, L. (2006). VS 30 mapping and soil classification for seismic site effect evaluation in Dinar region, SW Turkey. *Geophysical Journal International*, 165(1), 223-235.
- [2] Foti, S., Parolai, S., Albarello, D., & Picozzi, M. (2011). Application of surface-wave methods for seismic site characterization. *Surveys in geophysics*, 32, 777-825.
- [3] Picozzi, M., Strollo, A., Parolai, S., Durukal, E., Özel, O., Karabulut, S., ... & Erdik, M. (2009). Site characterization by seismic noise in Istanbul, Turkey. *Soil Dynamics and Earthquake Engineering*, 29(3), 469-482.
- [4] Ulusay, R., & Kuru, T. (2004). 1998 Adana-Ceyhan (Turkey) earthquake and a preliminary microzonation based on liquefaction potential for Ceyhan Town. *Natural Hazards*, 32, 59-88.
- [5] Pamuk, E., Özdağ, Ö. C., & Akgün, M. (2019). Soil characterization of Bornova Plain (Izmir, Turkey) and its surroundings using a combined survey of MASW and ReMi methods and Nakamura's (HVSr) technique. *Bulletin of Engineering Geology and the Environment*, 78, 3023-3035.
- [6] Pamuk, E., Özdağ, Ö. C., Tunçel, A., Özyalın, Ş., & Akgün, M. (2018). Local site effects evaluation for Aliğa/Izmir using HVSr (Nakamura technique) and MASW methods. *Natural Hazards*, 90, 887-899.
- [7] Salata, S., & Uzelli, T. (2022). Are Soil and Geology Characteristics Considered in Urban Planning? An Empirical Study in Izmir (Türkiye). *Urban Science*, 7(1), 5.
- [8] Gülkan, P., Çeken, U., Çolakoğlu, Z., Uğraş, T., Kuru, T., Apak, A., Anderson, J. G., Sucuoğlu, H., Çelebi, M., Akkar, D. S., Yazgan, U. & Denizlioğlu, A. Z. (2007). Enhancement of the national strong-motion network in Turkey. *Seismological Research Letters*, 78(4), 429-438.
- [9] Kurtuluş, C. & Bozkurt, A. (2016). Integration of geophysical and geotechnical investigations for Çayırhan town. *Journal of Applied Earthscience*, 8(2), 15-27.
- [10] Kurtuluş, C., Sertçelik, İ., Sertçelik, F., Livaoğlu, H., & Saş, C. (2020). Investigation of soil characterization in Hatay Province in Turkey by using Seismic Refraction, Multichannel Analysis of Surface Waves and Microtremor. *Earth Sciences Research Journal*, 24(4), 473-484.
- [11] BSSC (Building Seismic Safety Council) (2003). Recommended Provisions for Seismic Regulations for New Buildings and Other Structures and Accompanying Commentary and Maps. FEMA 450, Chapter 3, 17-49.
- [12] 12) CEN (European Committee for Standardization) (2003). Design of structures for earthquake resistance – part 1: general rules, seismic actions and rules for buildings, EN-1998- 2003, European Committee for Standardization, Brussels
- [13] TDBY Türkiye (2018). Deprem ve Bina Yönetmeliği, Resmî Gazete, Sayı:30364, 18 Mart.
- [14] Rodriguez-Marek, A., Bray, J. D. & Abrahamson, N. A. (2001). An empirical geotechnical site response procedure. *Earthquake Spectra*, 17(1), 65–87.
- [15] Tildy, P., Hermann, L., & Neduca, B. (2007, September). Problems and Possible Solutions of Geophysics in Eurocode 8 Based Soil Classification. In *Near Surface 2007-13th EAGE European Meeting of Environmental and Engineering Geophysics* (pp. cp-30). European Association of Geoscientists & Engineers.
- [16] Paliwal, M., Goswami, H., Ray, A., Bharati, A. K., Rai, R., & Khandelwal, M. (2022). Stability prediction of residual soil and rock slope using artificial neural network. *Advances in Civil Engineering*, 2022.
- [17] Mittal, M., Satapathy, S. C., Pal, V., Agarwal, B., Goyal, L. M., & Parwekar, P. (2021). Prediction of coefficient of consolidation in soil using machine learning techniques. *Microprocessors and Microsystems*, 82, 103830.
- [18] Jalal, F. E., Xu, Y., Iqbal, M., Javed, M. F., & Jamhiri, B. (2021). Predictive modeling of swell-strength of expansive soils using artificial intelligence approaches: ANN, ANFIS and GEP. *Journal of Environmental Management*, 289, 112420.
- [19] Pradeep, T., Bardhan, A., Burman, A., & Samui, P. (2021). Rock strain prediction using deep neural network and hybrid models of anfis and meta-heuristic optimization algorithms. *Infrastructures*, 6(9), 129.